Preferential Recruitment of Neutrophils into the Cerebellum and Brainstem Contributes to the Atypical Experimental Autoimmune Encephalomyelitis Phenotype

Yudong Liu, Andrew T. Holdbrooks, Gordon P. Meares, Jessica A. Buckley, Etty N. Benveniste, and Hongwei Qin

The JAK/STAT pathway is critical for development, regulation, and termination of immune responses, and dysregulation of the JAK/STAT pathway, that is, hyperactivation, has pathological implications in autoimmune and neuroinflammatory diseases. Suppressor of cytokine signaling 3 (SOCS3) regulates STAT3 activation in response to cytokines that play important roles in the pathogenesis of neuroinflammatory diseases, including IL-6 and IL-23. We previously demonstrated that myeloid lineage–specific deletion of SOCS3 resulted in a severe, nonresolving atypical form of experimental autoimmune encephalomyelitis (EAE), characterized by lesions, inflammatory infiltrates, elevated STAT activation, and elevated cytokine and chemokine expression in the cerebellum. Clinically, these mice exhibit ataxia and tremors. In this study, we provide a detailed analysis of this model, demonstrating that the atypical EAE observed in LysMCre-SOCS3$^{fl/fl}$ mice is characterized by extensive neutrophil infiltration into the cerebellum and brainstem, increased inducible NO synthase levels in the cerebellum and brainstem, and prominent axonal damage. Importantly, infiltrating SOCS3-deficient neutrophils produce high levels of CXCL2, CCL2, CXCL10, NO, TNF-α, and IL-1β. Kinetic studies demonstrate that neutrophil infiltration into the cerebellum and brainstem of LysMCre-SOCS3$^{fl/fl}$ mice closely correlates with atypical EAE clinical symptoms. Ab-mediated depletion of neutrophils converts the atypical phenotype to the classical EAE phenotype and, in some cases, a mixed atypical/classical phenotype. Blocking CXCR2 signaling ameliorates atypical EAE development by reducing neutrophil infiltration into the cerebellum/brainstem. Thus, neutrophils lacking SOCS3 display elevated STAT3 activation and expression of proinflammatory mediators and play a critical role in the development of atypical EAE. ***The Journal of Immunology*****, 2015, 195: 841–852.**

Multiple sclerosis (MS) and experimental autoimmune encephalomyelitis (EAE), the most extensively studied mouse model of MS, are considered T cell–mediated demyelinating diseases of the CNS (1). It is now appreciated that myeloid cells, including dendritic cells, macrophages/monocytes, and activated microglia, as well as astrocytes, are important components of disease initiation and progression (2–6). Increasing evidence suggests an important role of neutrophils in MS/EAE. In EAE, neutrophils facilitate disease development in both the initiation phase and effector phase (7–11). CXCR2 signaling in neutrophils plays a pivotal role in this process, as blockade of CXCR2 signaling abrogates blood-brain barrier breakdown, CNS infiltration by leukocytes, and the development of clinical symptoms (8, 9). In the cuprizone-induced demyelination model, mice lacking CXCR2 are resistant to demyelination, and adoptive transfer of CXCR2-positive neutrophils into CXCR2$^{-/-}$ mice reverses this protection (12). CXCR2 ligands, CXCL1 and CXCL2, are C-X-C chemokines with potent chemotactic properties for neutrophils, and expression of these two chemokines is increased with EAE disease development (8, 13, 14). In MS patients, neutrophils exhibit a primed state with reduced apoptosis; higher expression of TLR2, fMLP receptor, IL-8R, and CD43; and enhanced degranulation and oxidative burst (15). Neutrophil-attracting chemokines such as IL-8 (murine homolog of CXCL1 and CXCL2) are found in the cerebrospinal fluid of opticospinal and conventional Asian MS patients, indicating the important involvement of these chemokines in the pathogenesis of MS (16). In addition, neutrophil infiltration is prominent in early active demyelinating spinal cord (SC) lesions of neuromyelitis optica patients (17). Furthermore, a recent study demonstrated that systemic expression of neutrophil-associated factors, including CXCL1, CXCL5, and neutrophil elastase, correlated with measures of MS lesion burden and clinical disability (18), further supporting the involvement of neutrophils in neuroinflammatory diseases.

MS is a heterogeneous disease in terms of inflammatory lesions (19, 20). For example, most MS patients have lesions in the brain with little SC involvement (19, 20). However, a small number of patients have lesions in the SC and optic nerves (opticospinal MS)

Department of Cell, Developmental and Integrative Biology, The University of Alabama at Birmingham, Birmingham, AL 35294

Received for publication December 9, 2014. Accepted for publication May 22, 2015.

This work was supported in part by National Institutes of Health Grant NS45290 (to E.N.B.), National Multiple Sclerosis Society Grants CA-1059-A-13 and RG-4885-A-14 (to E.N.B.), and National Multiple Sclerosis Society Career Transition Award TA3050-A-1 (to G.P.M.).

Address correspondence and reprint requests to Dr. Hongwei Qin or Dr. Etty N. Benveniste, Department of Cell, Developmental and Integrative Biology, The University of Alabama at Birmingham, 1918 University Boulevard, MCLM 390, Birmingham, AL 35294 (H.Q.) or Department of Cell, Developmental, and Integrative Biology, University of Alabama at Birmingham, 1900 University Boulevard, THT 926A, Birmingham, AL 35294 (E.N.B.). E-mail addresses: hqin@uab.edu (H.Q.) or tika@uab.edu (E.N.B.)

The online version of this article contains supplemental material.

Abbreviations used in this article: BM, bone marrow; BS, brainstem; CRB, cerebellum; EAE, experimental autoimmune encephalomyelitis; iNOS, inducible NO synthase; MOG, myelin oligodendrocyte glycoprotein; MS, multiple sclerosis; SC, spinal cord; SOCS3, suppressor of cytokine signaling 3; SP, spleen.

(16, 21). Thus, it is important to determine the mechanism(s) that leads to different sites of lesion localization, as this may tailor current therapies to individualized treatments. The spatial distribution of lesions has also been observed in EAE models. In classical EAE, lesions are predominantly localized in the SC (22), although inflammatory changes in the brainstem (BS) and cerebellum (CRB) are also observed, whereas, in atypical EAE models, inflammatory demyelination is predominantly in the CRB and BS (23–27). Therefore, determining the mechanisms that influence brain versus SC inflammation is clinically relevant, as most MS patients have lesions in the brain.

We previously demonstrated that mice with a specific deletion of the suppressor of cytokine signaling 3 (SOCS3) gene in myeloid cells (LysMCre-SOCS3$^{fl/fl}$) develop early onset of a severe and nonresolving disease with features of atypical EAE, which is characterized by involvement of the CRB, rather than the SC, and ataxia, significant weight loss, axial rotation, and tremors (3). Importantly, we found that there was a striking neutrophil infiltration in the brain. Of interest, several groups have reported other atypical EAE phenotypes in mice with dominant brain involvement and prominent neutrophil infiltration (23–27). Neutrophils are critical for recruiting mononuclear cells to various extravascular sites and initiating chronic inflammation. They produce a diverse array of proinflammatory mediators, including TNF-α, IL-1β, IL-6, IL-22, IL-23, IFN-γ, and IL-17A (11, 28–32). The potential of neutrophils in orchestrating mononuclear cell recruitment as well as their production of proinflammatory mediators may have important implications in the development of atypical EAE. The purpose of this study was to investigate the potential pathogenic role of neutrophils in atypical EAE development in LysMCre-SOCS3$^{fl/fl}$ mice.

Materials and Methods

Mice

SOCS3-floxed transgenic (SOCS3$^{fl/fl}$) mice (33) were a gift of W. Alexander (Walter and Eliza Hall Institute of Medical Research, Victoria, Australia), and were bred at University of Alabama at Birmingham. SOCS3 conditional knockout (LysMCre-SOCS3$^{fl/fl}$) mice were generated by serial breeding of SOCS3$^{fl/fl}$ mice with mice expressing Cre-recombinase under the control of the LysM promoter (3). All experiments were reviewed and approved by the institutional animal care and use committee of University of Alabama at Birmingham.

Peptides, Abs, and cytokines

Myelin oligodendrocyte glycoprotein $(MOG)_{35–55}$ peptide was synthesized by New England Peptide. LPS was from Sigma-Aldrich. Abs against murine CD11b, CD45, Ly-6C, Ly-6G, and TNF-α used for flow cytometry were from BioLegend. Ab against murine p-STAT3 used for flow cytometry was from Cell Signaling. Abs against inducible NO synthase (iNOS) and CCL2 used for flow cytometry were from BD Biosciences. LIVE/DEAD Fixable Aqua Stain kit was from Invitrogen. Ab against SMI-32 was from Covance, and Ab against GAPDH was from Abcam. Neutralizing anti–Ly-6G Ab (clone 1A8) and isotype control Ab (rat IgG2a, clone 2A3) were from Bio X Cell (West Lebanon, NH). CXCR2 antagonist SB 225002 was from Cayman Chemical (Ann Arbor, MI).

EAE induction and assessment

Active EAE was induced as previously described (3, 34). Eight- to 12-wk-old SOCS3$^{fl/fl}$ or LysMCre-SOCS3$^{fl/fl}$ mice were immunized s.c. with 100 μg $MOG_{35–55}$ emulsified in CFA (supplemented with 2 mg/ml *Mycobacterium tuberculosis*) and injected i.p. on days 0 and 2 with 500 ng pertussis toxin. Assessment of classical EAE was as follows: 0, no disease; 1, decreased tail tone; 2, hind limb weakness or partial paralysis; 3, complete hind limb paralysis; 4, front and hind limb paralysis; and 5, moribund state. Assessment of atypical EAE was as follows: 0, no disease; 1, hunched appearance, stiff tail; 2, staggered walking, scruffy coat; 3, head tilt, ataxia, obvious impaired balance/ambulation, body lean; 4, inability to maintain upright posture, severe axial rotation, severe body lean; and 5, moribund. Mixed EAE was defined as mice that exhibited both classical and atypical symptoms. All mice were scored by the two scoring systems separately. For neutrophil depletion, mice were treated i.p. at the indicated time points with 200 μg anti–Ly-6G or isotype control. For CXCR2 blockage, SB 225002, a selective nonpeptide inhibitor of CXCR2 (dissolved in 10% DMSO, 5% Tween 20, 10% PEG 400, 75% saline, and 200 μg/mouse) (35), or vehicle control was administered i.p. at the indicated time points. Mice were sacrificed and perfused, and mononuclear cells were isolated from the CNS (CRB, BS, and SC) by a 30/70% Percoll gradient, or from draining cervical lymph nodes and spleen (SP), and cell phenotype was determined by surface and intracellular staining by flow cytometry, as previously described (3, 34).

Preparation of neutrophils from bone marrow and blood

Total bone marrow (BM) cells were recovered from the femur and tibia by flushing with RPMI 1640 medium with an 18-gauge needle, and RBCs were lysed. Blood was collected, serum was removed, and RBCs were lysed. Then cells from BM and blood were stained with CD45, CD11b, Ly-6G, and Ly-6C, and neutrophils were sorted as $CD45^+CD11b^+Ly\text{-}6C^-Ly\text{-}6G^+$.

Flow cytometry

Neutrophils were stimulated for 4 h with LPS (10 ng/ml) plus GolgiStop (BD Pharmingen) and were analyzed for intracellular production of TNF-α and CCL2. For iNOS-producing neutrophils, cells were fixed with 4% paraformaldehyde after surface staining for CD45, CD11b, Ly-6C, and Ly-6G, followed by 90% methanol permeabilization and intracellular staining with anti-iNOS Ab. Cells were acquired on a LSRII flow cytometer (BD Biosciences, San Jose, CA), and data were analyzed using FlowJo software (Tree Star, Ashland, OR).

Immunohistology analysis

Mice were transcardially perfused with ice-cold PBS and 4% paraformaldehyde in PBS under deep anesthesia. CNS tissues were postfixed in the same fixative overnight at 4°C, followed by cryoprotection in 30% (w/v) sucrose in PBS overnight at 4°C. Cryoprotected brains were embedded in Optimal Cutting Temperature compound (Fisher Scientific) and cryosectioned at 8 μm. Sections were stained with H&E and/or immunofluorescence. For immunofluorescence, sections were rinsed in PBS, permeabilized with 0.4% Triton X-100, blocked with 10% donkey serum, and then incubated in a mixture of primary Abs diluted in PBS containing 2% donkey serum and 0.1% Triton X-100 overnight at 4°C. The sections were washed extensively with PBS and then incubated for 30 min at room temperature in species-specific secondary Abs (all raised in donkey) conjugated to Alexa Fluor 488 or Alexa Fluor 596. Sections were washed again and mounted using Prolong antifade medium (Invitrogen). All fluorescent and confocal images were acquired with an Olympus FV1000 Laser Confocal Scanning microscope and were subsequently analyzed using the FV10-ASW software. Images were collected at the same time using identical settings with respect to image exposure time and image compensation settings, as described (3).

Nitrite assay

Supernatants were collected and analyzed for nitrite, a stable end product of NO, using the Griess reaction, as previously described (36). Briefly, 50 μl supernatant was incubated with 50 μl Griess reagent in 96-well flat-bottom tissue culture plates. Samples were then read at 540 nm to measure nitrite levels.

RNA isolation, RT-PCR, and TaqMan gene expression assays

Total RNA was isolated from the CRB, BS, and SC of mice, and reverse-transcriptase reactions were performed, as described (3, 34). Five hundred nanograms RNA was used to reverse transcribe into cDNA and subjected to quantitative RT-PCR. The data were analyzed using the comparative cycle threshold method to obtain relative quantitation values.

Immunoblotting

Total of 40 μg cell lysate or brain homogenate was separated by electrophoresis and probed with Abs, as described previously (3, 34).

Statistical analysis

Levels of significance for comparison between two groups were determined by one-sided two-sample Mann–Whitney rank sum test and the Student *t* test distribution. A p value <0.05 was considered statistically significant.

Results

Mice with deletion of SOCS3 in myeloid cells develop atypical EAE that mainly affects the CRB and BS

We first confirmed and extended our previous observation that mice with deletion of SOCS3 in cells of the myeloid lineage develop early onset of a severe and nonresolving disease with features of atypical EAE (3). As shown in Fig. 1A, pure atypical EAE symptoms were only observed in LysMCre-SOCS3$^{fl//fl}$ mice, and the majority of SOCS3$^{fl//fl}$ mice exhibited classical EAE symptoms. Interestingly, 23.1% of SOCS3$^{fl//fl}$ mice and 11.1% of LysMCre-SOCS3$^{fl//fl}$ mice developed a mixed phenotype, which is characterized by signs of atypical EAE accompanied by ascending paralysis. Next, we examined the pattern of mononuclear cell infiltration into different CNS compartments of SOCS3$^{fl//fl}$ mice that exclusively had classical EAE or of LysMCre-SOCS3$^{fl//fl}$ mice that exclusively had atypical EAE during disease development. We consistently observed a substantial mononuclear cell infiltration into the CRB and BS after onset of disease in LysMCre-SOCS3$^{fl//fl}$ mice with atypical EAE, with minimal mononuclear cell infiltration into the SC (Fig. 1B). In contrast, mononuclear cell infiltration into the SC of SOCS3$^{fl//fl}$ mice with classical EAE was observed (Fig. 1B). H&E staining also confirmed the increased level of mononuclear cells in the BS of LysMCre-SOCS3$^{fl//fl}$ mice compared with SOCS3$^{fl//fl}$ mice (Fig. 1C). Levels of proinflammatory mediators, including IL-1β, TNF-α, and iNOS, were examined in the different CNS compartments at different disease stages. Significantly increased levels of these proinflammatory mediators were detected in the CRB and, in some instances, the BS from LysMCre-SOCS3$^{fl//fl}$ mice with atypical EAE at ongoing and peak of disease compared with SOCS3$^{fl//fl}$ mice with classical EAE (Fig. 1D). Significantly increased levels of IL-1β and iNOS were also observed in the SC of LysMCre-SOCS3$^{fl//fl}$ mice with atypical EAE during ongoing disease, but no differences were observed at the peak of disease. When comparing the ratio of fold induction in these genes between CRB and SC or between BS and SC, significantly higher CRB/SC ratios and BS/SC ratios were observed in LysMCre-SOCS3$^{fl//fl}$ mice compared with SOCS3$^{fl//fl}$ mice (Supplemental Table I). These data confirm and extend our previous observations that atypical EAE in LysMCre-SOCS3$^{fl//fl}$ mice affects both CRB and BS and, in some instances, the SC, compared with classical EAE that mainly affects the SC in SOCS3$^{fl//fl}$ mice.

Neutrophil infiltration into the CRB and BS is prominent in atypical EAE

To determine the mechanisms that regulate development of atypical EAE versus classical EAE, we performed a detailed analysis of the cellular composition of leukocyte infiltration in different CNS compartments of SOCS3$^{fl//fl}$ mice that exclusively had classical EAE or LysMCre-SOCS3$^{fl//fl}$ mice that exclusively had atypical

A

	EAE Incidence			Disease Onset (d)	Disease Peak (d)
	Classical %	Mixed %	Atypical %		
SOCS3$^{fl/fl}$	76.9	23.1	0	9.6 ± 1.2	14.5 ± 0.8
LysMCre-SOCS3$^{fl/fl}$	0	11.1	88.9	7.8 ± 0.7	12.4 ± 1.0

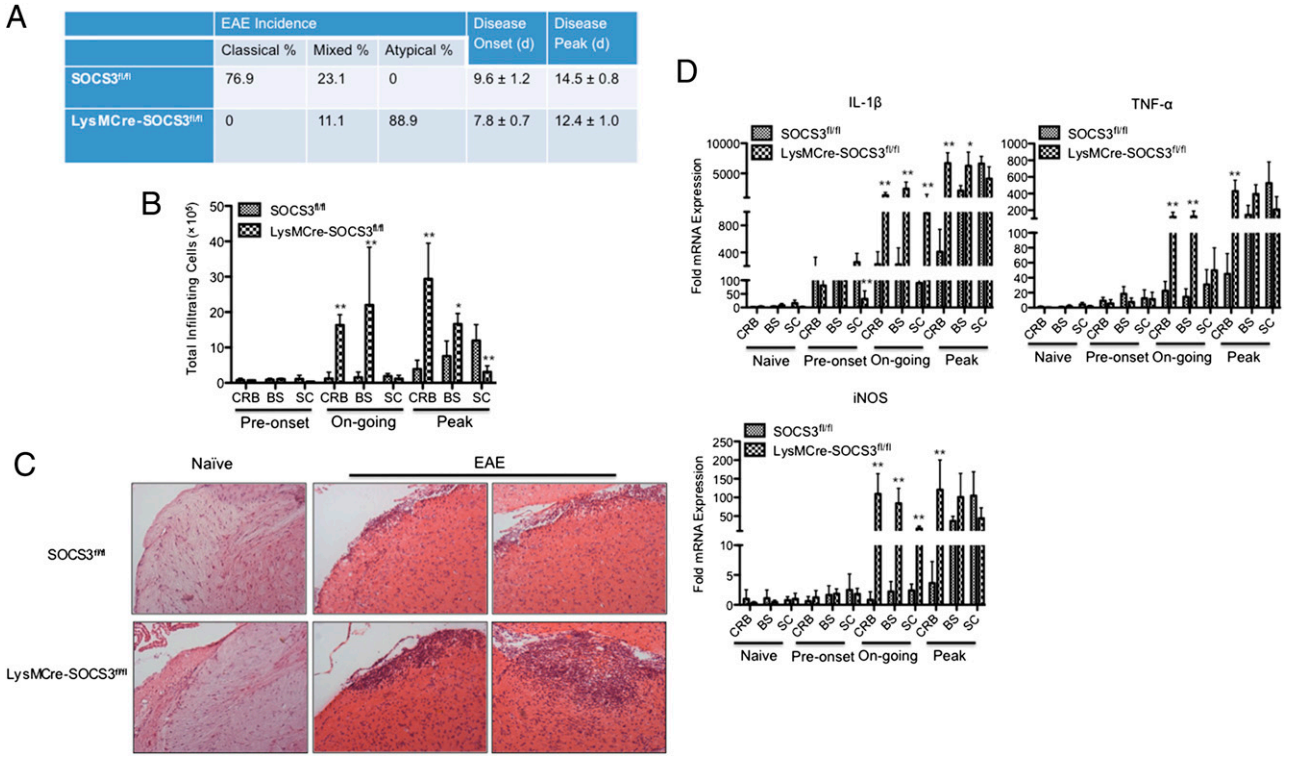

FIGURE 1. Deletion of SOCS3 in myeloid cells causes atypical EAE. (**A**) SOCS3$^{fl/fl}$ ($n = 26$) or LysMCre-SOCS3$^{fl/fl}$ ($n = 36$) mice were immunized with $MOG_{35–55}$ peptide. The mice received i.p. injections of 500 ng pertussis toxin on days 0 and 2. Data were pooled from at least five experiments. (**B**) Representative graph illustrating quantitative data for absolute numbers of total infiltrating mononuclear cells in the CRB, BS, and SC from SOCS3$^{fl//fl}$ mice with classical EAE or from LysMCre-SOCS3$^{fl//fl}$ mice with atypical EAE during disease development. Preonset (clinical scores of 0–1 at days 9–10 for classical EAE in SOCS3$^{fl/fl}$ mice or at days 5–6 for atypical EAE in LysMCre-SOCS3$^{fl//fl}$ mice), ongoing (clinical scores of 1–3 at days 11–13 for classical EAE in SOCS3$^{fl/fl}$ mice or at days 7–10 for atypical EAE in LysMCre-SOCS3$^{fl//fl}$ mice), and peak (clinical scores of 3–4 in classical EAE at days 14–18 for classical EAE in SOCS3$^{fl/fl}$ mice or at days 11–15 for atypical EAE in LysMCre-SOCS3$^{fl//fl}$ mice). Mean ± SD numbers of total infiltrating cells in different CNS compartments were compared between SOCS3$^{fl/fl}$ and LysMCre-SOCS3$^{fl/fl}$ mice. (**C**) H&E staining of BS sections at the peak of disease from SOCS3$^{fl/fl}$ mice with classical EAE or LysMCre-SOCS3$^{fl/fl}$ mice with atypical EAE, as well as BS sections from naive SOCS3$^{fl/fl}$ and LysMCre-SOCS3$^{fl/fl}$ mice (original magnification ×10). Representative sections from each group are shown. (**D**) CRB, BS, and SC mRNA were isolated at the indicated disease stages for RT-PCR analysis of IL-1β, TNF-α, and iNOS. Data represent fold induction compared with naive SOCS3$^{fl/fl}$ CRB. Fold induction of indicated genes in different CNS compartments was compared between SOCS3$^{fl/fl}$ and LysMCre-SOCS3$^{fl/fl}$ mice at the indicated disease stages. *$p < 0.05$, **$p < 0.01$.

EAE, with an emphasis on myeloid cells. Importantly, we found a much higher percentage of neutrophils ($CD45^+CD11b^+Ly\text{-}6C^{low}$ $Ly\text{-}6G^+$) in total CNS-infiltrating mononuclear cells ($CD45^+$ cells) in the CRB and BS, but not in the SC in LysMCre-$SOCS3^{fl//fl}$ mice with atypical EAE compared with $SOCS3^{fl//fl}$ mice with classical EAE (Fig. 2A). The presence of neutrophils in the CRB was also confirmed by morphological analysis (Fig. 2B), and neutrophils within the CRB and BS were confirmed by immunohistochemical staining for expression of the neutrophil-specific marker Ly-6G (Fig. 2C). Next, we assessed the kinetics of neutrophil infiltration into different CNS compartments during EAE development. Interestingly, at preonset of disease, modest neutrophil infiltration was observed in all CNS compartments in both $SOCS3^{fl//fl}$ mice with classical EAE and LysMCre-$SOCS3^{fl//fl}$ mice with atypical EAE (Fig. 2D). However, during ongoing and peak disease, there was a striking increase in neutrophil infiltration in the CRB and BS of LysMCre-$SOCS3^{fl//fl}$ mice (Fig. 2D), and the levels of neutrophils directly correlated with atypical EAE clinical symptom development. In contrast, neutrophil levels decreased in the CRB, and to a lesser extent, in the BS, of $SOCS3^{fl//fl}$ mice during classical EAE development (Fig. 2D). The level of neutrophils in the SC was similar between $SOCS3^{fl//fl}$ mice and LysMCre-$SOCS3^{fl//fl}$ mice (Fig. 2D). More importantly, the ratio of the percentage of neutrophils to percentage of macrophages/monocytes in the CRB and BS was significantly higher in LysMCre-$SOCS3^{fl//fl}$ mice compared with $SOCS3^{fl//fl}$ mice (Fig. 2E). These data indicate an increase of neutrophil frequency as well as a higher ratio of the percentage of neutrophils to percentage of macrophages/monocytes in the CRB and BS, which closely correlates with the clinical course of atypical EAE.

Increased levels of neutrophil- and macrophage/monocyte-attracting chemokines in the CRB and BS in LysMCre-$SOCS3^{fl//fl}$ mice with atypical EAE

CXCL1, CXCL2, and CCL2 are potent neutrophil and macrophage chemoattractants (8, 37, 38). Given the increased levels of neutrophils and macrophages/monocytes infiltrating into the CRB and BS in LysMCre-$SOCS3^{fl//fl}$ mice with atypical EAE compared with $SOCS3^{fl//fl}$ mice with classical EAE (although the increase of neutrophils is more prominent than that of macrophages/monocytes in LysMCre-$SOCS3^{fl//fl}$ mice), we determined the expression pattern of these chemokines in the different CNS com-

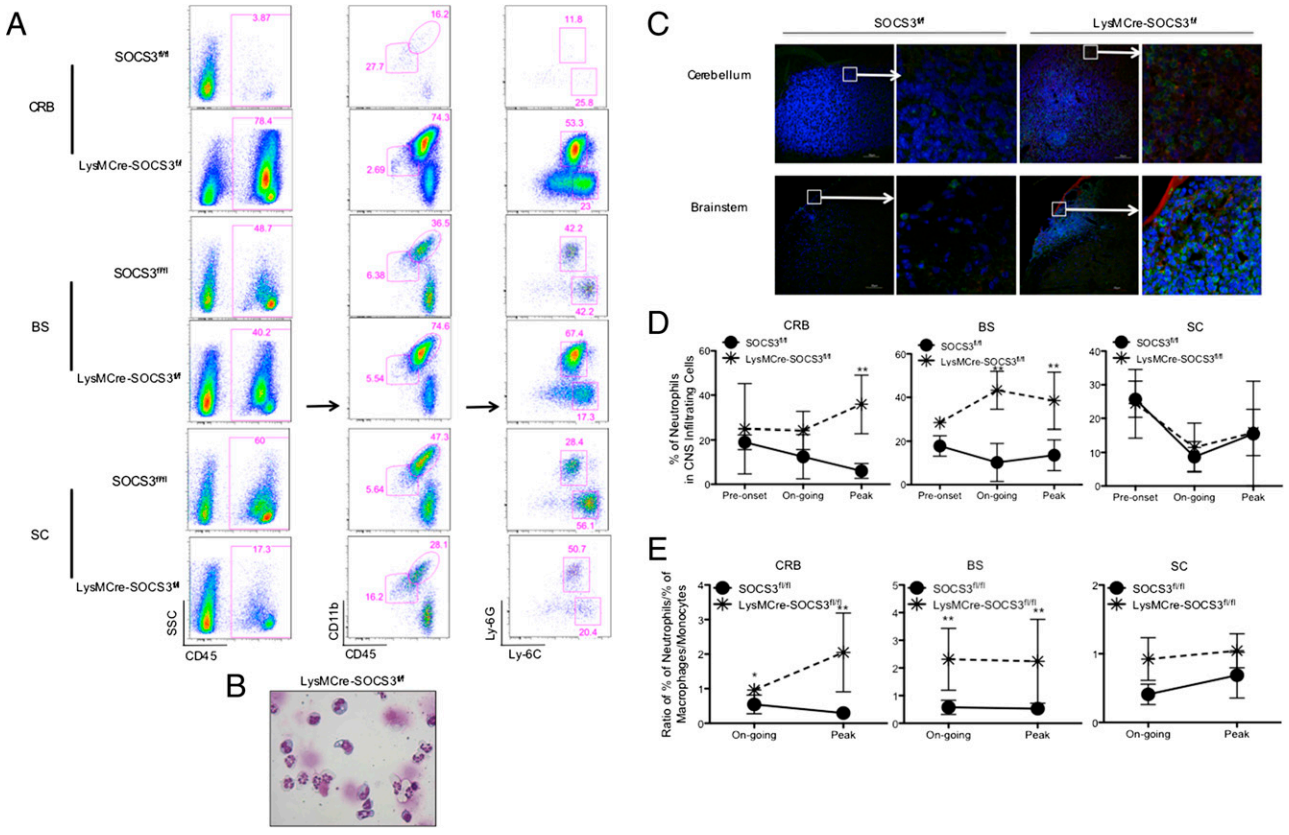

FIGURE 2. Neutrophil infiltration into the CRB and BS is prominent in atypical EAE. (**A**) CRB-, BS-, and SC-infiltrating mononuclear cells were isolated from $SOCS3^{fl/fl}$ mice with classical EAE (score of 3) or from LysMCre-$SOCS3^{fl/fl}$ mice with atypical EAE (score of 3). They were first gated on $CD45^+$, and then gated on CD11b, Ly-6C, and Ly-6G. Representative flow cytometry plot of neutrophils is shown (n = 10 mice/group). Neutrophils were defined as $CD45^+CD11b^+Ly\text{-}6C^{low}Ly\text{-}6G^+$, and macrophages/monocytes were defined as $CD45^+CD11b^+Ly\text{-}6C^{high}Ly\text{-}6G^-$. (**B**) CRB-infiltrating mononuclear cells isolated from LysMCre-$SOCS3^{fl/fl}$ mice at the peak of atypical EAE were cytospinned, and slides were stained with Diff Quik. (**C**) Immunohistochemistry staining of CRB and BS sections at peak of disease from $SOCS3^{fl/fl}$ mice with classical EAE or LysMCre-$SOCS3^{fl/fl}$ mice with atypical EAE. Sections were stained with Ly-6G Ab (green), SMI-32 Ab (red), and Hoechst (blue). Representative sections from each group are shown (n = 4 mice/group). Bar size of 30 μm is shown. (**D**) Representative graph of three individual experiments illustrating quantitative data for percentage of accumulated neutrophils in total CNS-infiltrating cells from CRB, BS, and SC at the indicated clinical phases from $SOCS3^{fl/fl}$ mice with classical EAE or LysMCre-$SOCS3^{fl/fl}$ mice with atypical EAE (n = 3 mice/group). Mean ± SD. Percentage of neutrophils in CNS-infiltrating cells in different CNS compartments was compared between $SOCS3^{fl/fl}$ and LysMCre-$SOCS3^{fl/fl}$ mice at the indicated disease stages. (**E**) Representative graph from three individual experiments illustrating ratio of percentage of accumulated neutrophils to percentage of accumulated macrophages/monocytes from the CRB, BS, and SC at the indicated clinical phases from $SOCS3^{fl/fl}$ mice with classical EAE or LysMCre-$SOCS3^{fl/fl}$ mice with atypical EAE. Mean ± SD (n = 3 mice/group). $^*p < 0.05$, $^{**}p < 0.01$.

partments throughout the course of disease. A significant increase in CXCL1 expression was observed in all CNS compartments in LysMCre-SOCS3$^{fl//fl}$ mice starting at preonset of disease and was maintained throughout the course of disease, although levels were higher in the CRB compared with BS and SC at the peak of disease (Fig. 3A). The levels of CXCL1 were moderately increased in SOCS3$^{fl//fl}$ mice. Interestingly, expression of CXCL2 and CCL2 in all CNS compartments from LysMCre-SOCS3$^{fl//fl}$ mice was slightly increased at preonset of disease, and then increased at later time points (Fig. 3A). Importantly, significantly higher levels of CXCL2 and CCL2 expression were found in the CRB and BS in LysMCre-SOCS3$^{fl//fl}$ mice with atypical EAE compared with SOCS3$^{fl//fl}$ mice with classical EAE during ongoing and peak of disease (Fig. 3A). When comparing CXCL2 and CCL2 expression levels between CRB and SC, or between BS and SC, ratios were significantly higher in LysMCre-SOCS3$^{fl//fl}$ mice (Supplemental Table I), further confirming that atypical EAE is mainly affecting the brain. We also confirmed significantly higher levels of CXCL2 and CCL2 protein in the CRB and BS from LysMCre-SOCS3$^{fl//fl}$ mice by ELISA (Fig. 3B).

As the kinetics of CXCL2 and CCL2 expression levels paralleled the kinetics of mononuclear cell infiltration into the CRB and BS, we determined whether these CNS-infiltrating cells contributed to the increased levels of these chemokines. Mononuclear cells isolated from the CRB, BS, and SC of SOCS3$^{fl/fl}$ mice and LysMCre-SOCS3$^{fl/fl}$ mice at the peak of classical EAE or atypical EAE, respectively, were cultured for 24 h, and supernatants were assayed for CXCL2 and CCL2. We observed a significant increase of CXCL2 and CCL2 levels in the supernatants from cultured CRB-infiltrating mononuclear cells from LysMCre-SOCS3$^{fl/fl}$ mice compared with SOCS3$^{fl/fl}$ mice (Fig. 3C). In contrast, significantly higher levels of CXCL2 and CCL2 from cultured SC-infiltrating mononuclear cells from SOCS3$^{fl/fl}$ mice were detected (Fig. 3C).

Neutrophil depletion converts the atypical phenotype to mixed and classical phenotypes

Our findings to date suggest that preferential neutrophil recruitment to the CRB and BS correlates with the development of atypical EAE. To further assess the functional relevance of neutrophils in the pathogenesis of atypical EAE, we administered the neutrophil-specific anti–Ly-6G Ab (clone 1A8), which has been widely used to deplete neutrophils in vivo (26, 27), beginning on the day of MOG immunization. As reported, injection of 1A8 Ab displayed efficacy in depleting circulating neutrophils without affecting other leukocyte populations (Supplemental Fig. 1). Importantly, we observed that low levels of neutrophils were maintained for at least 3 d after Ab injection (Supplemental Fig. 1). Treatment of

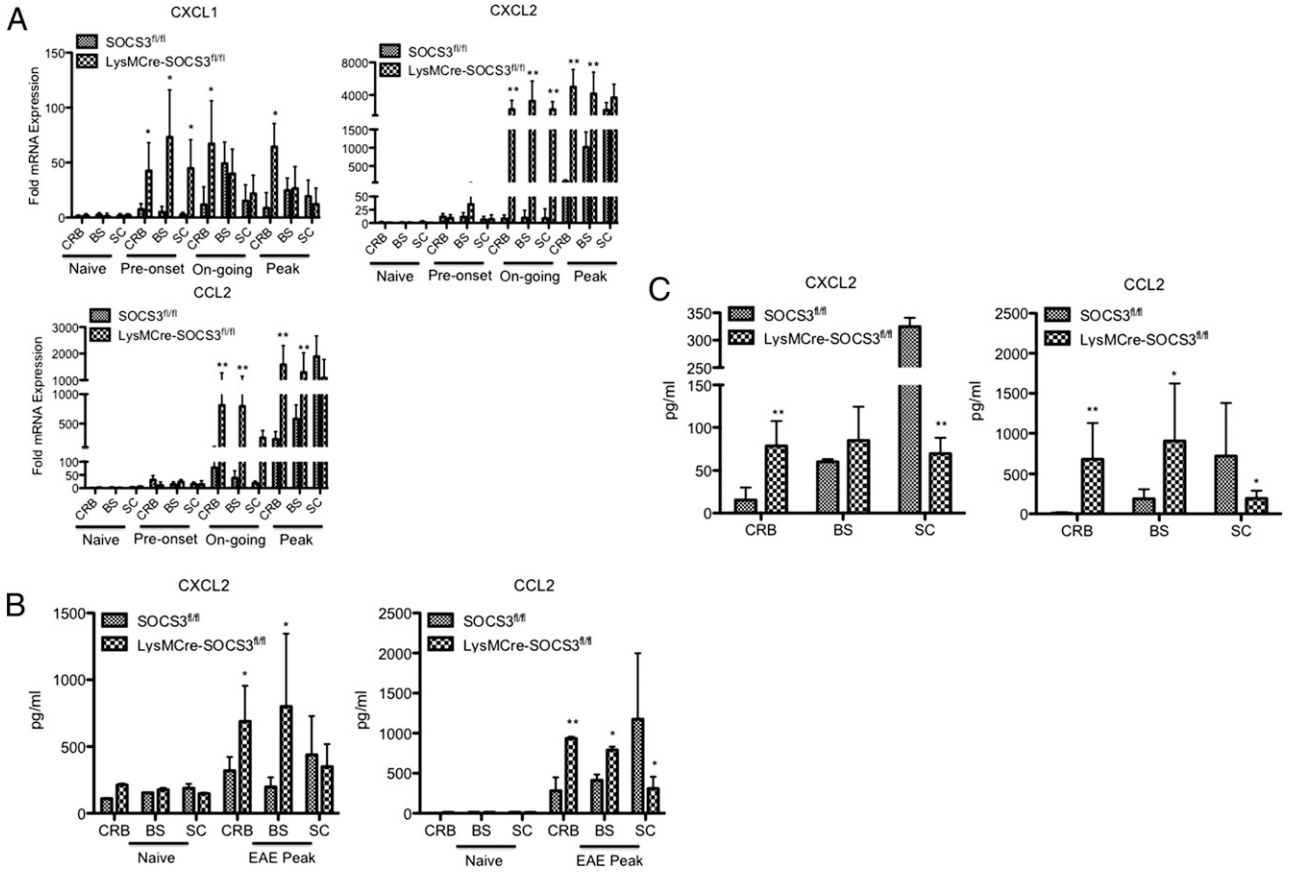

FIGURE 3. Increased levels of neutrophil- and macrophage/monocyte-attracting chemokines in the CRB and BS in LysMCre-SOCS3$^{fl//fl}$ mice with atypical EAE. (**A**) SOCS3$^{fl//fl}$ or LysMCre-SOCS3$^{fl/fl}$ mice were immunized with $MOG_{35–55}$ peptide. CRB, BS, and SC mRNA were isolated at the indicated disease stages for RT-PCR analysis of CXCL1, CXCL2, and CCL2. Data represent fold induction compared with naive SOCS3$^{fl/fl}$ CRB (n = 3 mice/group). Data represent three individual experiments. (**B**) Supernatants obtained from CRB, BS, and SC homogenates at the peak of disease from SOCS3$^{fl/fl}$ mice with classical EAE or LysMCre-SOCS3$^{fl/fl}$ mice with atypical EAE were subjected to ELISA for CXCL2 and CCL2. Levels of indicated protein in different CNS compartments were compared between SOCS3$^{fl/fl}$ and LysMCre-SOCS3$^{fl/fl}$ mice at the indicated disease stages (n = 5 mice/group). (**C**) Total CRB-, BS-, and SC-infiltrating mononuclear cells isolated at the peak of disease from SOCS3$^{fl/fl}$ mice with classical EAE or from LysMCre-SOCS3$^{fl/fl}$ mice with atypical EAE were cultured for 24 h, and supernatants were analyzed for CXCL2 and CCL2 by ELISA. Mean ± SD. Levels of indicated protein in different CNS compartments were compared between SOCS3$^{fl/fl}$ and LysMCre-SOCS3$^{fl/fl}$ mice (n = 4 mice/group). *$p < 0.05$, **$p < 0.01$.

LysMCre-SOCS3$^{fl//fl}$ mice with 1A8 Ab significantly delayed atypical EAE onset (8.1 ± 0.7 versus 10.6 ± 1.3) and lessened atypical EAE clinical scores (Fig. 4A, 4B). Interestingly, neutrophil depletion significantly reduced the incidence of atypical EAE (from 90 to 14.3%) and significantly increased the incidence of the classical phenotype (from 0 to 57.1%) (Fig. 4A, 4B). Concordant with the transition from the atypical phenotype to classical phenotype, 1A8 Ab treatment reduced mononuclear cell infiltration into the CRB, and significantly increased mononuclear cell infiltration into the SC (Fig. 4C). Importantly, 1A8 Ab treatment significantly reduced the level of neutrophils in the CRB (Fig. 4D). We also observed a trend of decreased levels of neutrophils in the BS (Fig. 4D). Expression levels of CXCL1, CXCL2, CCL2, IL-1β, CXCL10, and iNOS were significantly reduced in the CRB from 1A8 Ab-treated mice and, in some instances, the BS (Fig. 4E). Surprisingly, 1A8 Ab treatment had little effect on the development of classical EAE; however, the incidence of mixed phenotype was abrogated (Supplemental Fig. 2A, 2B). In addition, mononuclear cell infiltration into the CRB and BS was significantly reduced (Supplemental Fig. 2C). A trend of decreased percentage of neutrophils in the SC was also observed (Supplemental Fig. 2D).

Neutrophils are pathogenic in the development of atypical EAE by producing proinflammatory chemokines and cytokines

During EAE development, the interplay between CNS-resident cells and CNS-infiltrating cells generates a unique inflammatory microenvironment in the brain, which may be different from that in the periphery. A number of studies document that neutrophils produce a diverse array of proinflammatory mediators, including CXCL2, CCL2, TNF-α, IL-1β, and iNOS (11, 28, 39–41). As we observed a close correlation between the kinetics of expression of proinflammatory chemokines and cytokines and the kinetics of CRB- and BS-infiltrating neutrophils, we focused on the gene expression profiles of these chemokines and cytokines in neutrophils. We previously showed that neutrophils from LysMCre-SOCS3$^{fl//fl}$ mice are deficient in the *socs3* gene (3), and this deletion leads to enhanced and prolonged activation of STAT3 in response to stimuli such as G-CSF (Fig. 5A), as well as other stimuli such as IL-6 (3). SOCS3-deficient neutrophils were sorted (CD45$^+$CD11b$^+$Ly-6C^{low}Ly-6G$^+$) from mononuclear cells isolated from CRB, BS, and SP of LysMCre-SOCS3$^{fl/fl}$ mice at the peak of atypical EAE or from SP of naive LysMCre-SOCS3$^{fl/fl}$ mice, and

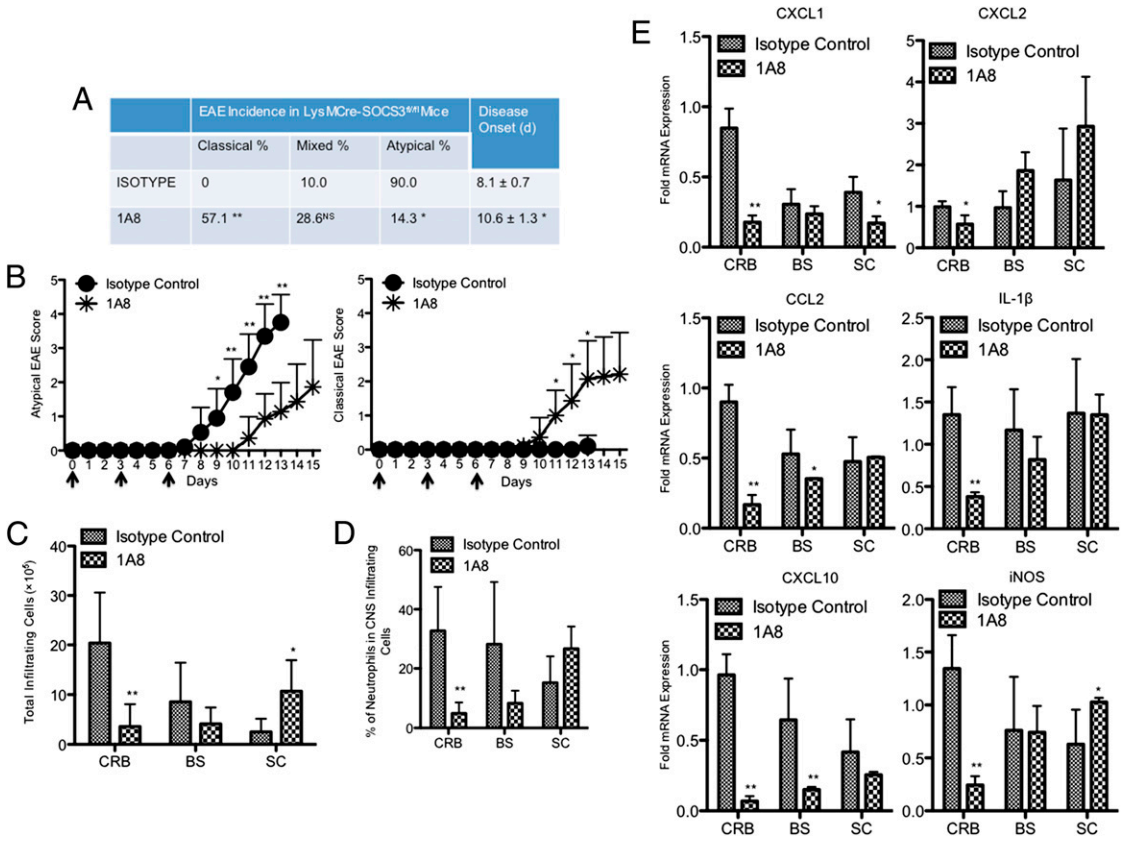

FIGURE 4. Neutrophil depletion converts the atypical phenotype to mixed and classical phenotypes. (**A**) LysMCre-SOCS3$^{fl/fl}$ mice were administered 200 μg 1A8 Ab (n = 21) or isotype control Ab (n = 20) i.p. on days 0, 3, and 6 postimmunization. Data were pooled from at least three experiments. Incidence of different EAE phenotypes and day of disease onset were compared between isotype control group and 1A8 group. (**B**) Mean ± SD of atypical and classical EAE scores. Data were pooled from at least three experiments. Atypical EAE scores or classical EAE scores were compared between isotype control group and the 1A8-treated group at the indicated time points. (**C**) Representative graph illustrating quantitative data for absolute numbers of total infiltrating mononuclear cells in the CRB, BS, and SC from LysMCre-SOCS3$^{fl//fl}$ mice treated with isotype control or 1A8 Ab at the peak of disease. Mean ± SD. Numbers of total infiltrating cells in different CNS compartments were compared between isotype control group or 1A8 group. (**D**) Representative graph illustrating quantitative data for percentage of accumulated neutrophils in total CNS-infiltrating cells from CRB, BS, and SC from LysMCre-SOCS3$^{fl//fl}$ mice treated with isotype control or 1A8 Ab at the peak of disease. Mean ± SD. Percentage of neutrophils in CNS-infiltrating cells in different CNS compartments were compared between isotype control group and 1A8 group. (**E**) CRB, BS, and SC mRNA were isolated from LysMCre-SOCS3$^{fl//fl}$ mice treated with isotype control or 1A8 Ab at the peak of disease for RT-PCR analysis of CXCL1, CXCL2, CCL2, IL-1β, CXCL10, and iNOS. Data represent fold induction compared with isotype control CRB. Fold induction of indicated genes in different CNS compartments was compared between isotype control group and 1A8 group. *$p < 0.05$, **$p < 0.01$.

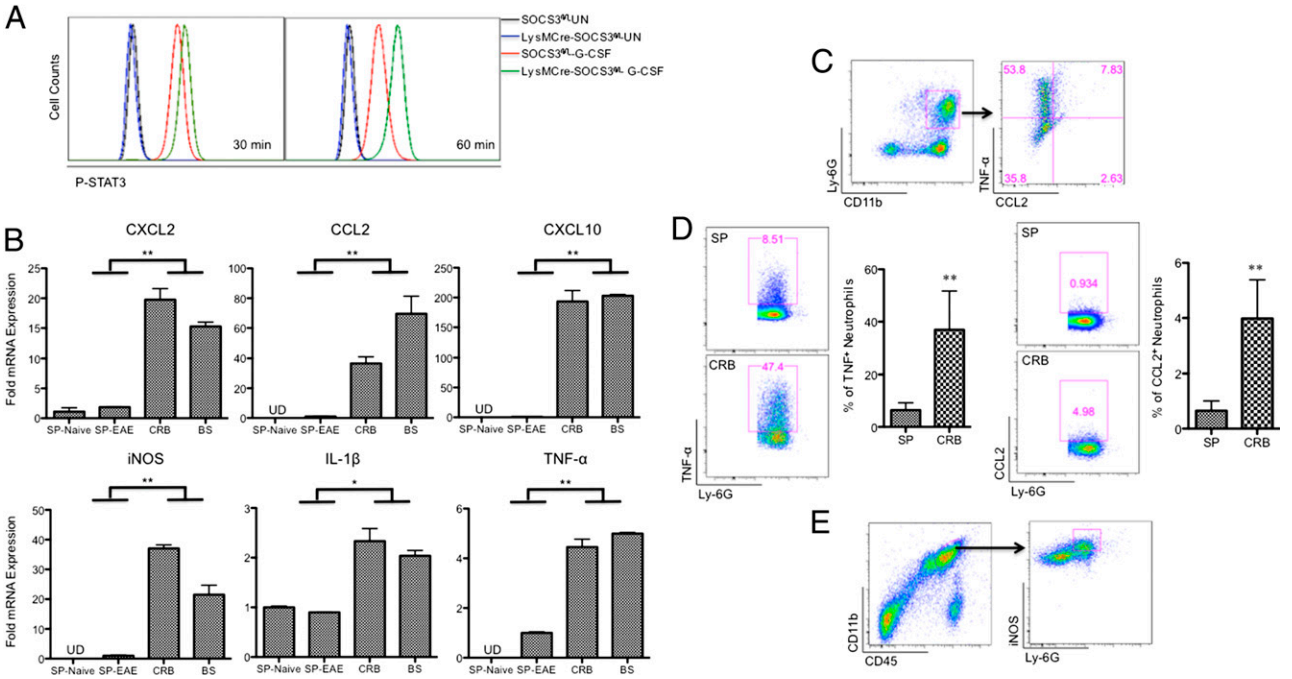

FIGURE 5. Neutrophils are pathogenic in the development of atypical EAE by producing proinflammatory chemokines and cytokines. (**A**) Cells from the bone marrow of SOCS3$^{fl/fl}$ or LysMCre-SOCS3$^{fl/fl}$ mice were treated with G-CSF (10 ng/ml) for 30 and 60 min, and then cells were stained with Abs to CD11b, Ly-6G, and p-STAT3. (**B**) CD45^{+}CD11b^{+}Ly-6C^{low}Ly-6G^{+} neutrophils were sorted from splenocytes of naive LysMCre-SOCS3$^{fl/fl}$ mice or from splenocytes and CRB- and BS-infiltrating mononuclear cells at the peak of disease from LysMCre-SOCS3$^{fl/fl}$ mice with atypical EAE ($n = 4$ mice). mRNA was isolated and analyzed for CXCL2, CCL2, CXCL10, iNOS, IL-1β, and TNF-α. Mean ± SD. Data represent fold induction compared with neutrophils isolated from naive LysMCre-SOCS3$^{fl/fl}$ splenocytes. Fold induction of indicated genes was compared between CRB- and BS-infiltrating neutrophils and neutrophils from SP of naive mice or EAE mice. Data represent three individual experiments. (**C**) CRB-infiltrating mononuclear cells isolated from LysMCre-SOCS3$^{fl/fl}$ mice at the peak of atypical EAE were stimulated in the presence of LPS (10 ng/ml) with GolgiStop for 4 h and stained for the surface markers CD45, CD11b, Ly-6C, and Ly-6G (*left panel*), and by intracellular flow for TNF-α and CCL2 (*right panel*) ($n = 4$ mice). (**D**) CRB-infiltrating mononuclear cells and splenocytes isolated from LysMCre-SOCS3$^{fl/fl}$ mice at the peak of atypical EAE were stimulated in the presence of LPS (10 ng/ml) with GolgiStop for 4 h and stained for the surface markers CD45, CD11b, Ly-6C, and Ly-6G (*left panel*), and by intracellular flow for TNF-α (*left panel*) or CCL2 (*right panel*) ($n = 4$ mice). (**E**) CRB-infiltrating mononuclear cells isolated from LysMCre-SOCS3$^{fl/fl}$ mice at the peak of atypical EAE were stained with Abs to CD45, CD11b, Ly-6G, and iNOS. Cells were first gated on CD11b and CD45 (*left panel*), and then gated on Ly-6G and iNOS (*right panel*). Representative flow cytometry plot of iNOS^{+} neutrophils ($n = 4$ mice). $^{*}p < 0.05$, $^{**}p < 0.01$.

the sorted neutrophils were directly analyzed for mRNA expression. Importantly, we found that expression of CXCL2, CCL2, CXCL10, iNOS, IL-1β, and TNF-α was significantly increased in CRB- and BS-infiltrating SOCS3-deficient neutrophils compared with SOCS3-deficient neutrophils from SP from EAE mice or SP from naive mice (Fig. 5B). Using flow cytometry, we confirmed the production of CCL2 and TNF-α by CRB-infiltrating SOCS3-deficient neutrophils from LysMCre-SOCS3$^{fl/fl}$ mice at the peak of atypical EAE (Fig. 5C). In addition, we confirmed higher levels of TNF-α and CCL2 on a per-cell basis in CRB-infiltrating neutrophils compared with SP-derived neutrophils from LysMCre-SOCS3$^{fl/fl}$ mice at the peak of atypical EAE (Fig. 5D). We also confirmed the production of iNOS by CRB-infiltrating SOCS3-deficient neutrophils from LysMCre-SOCS3$^{fl/fl}$ mice at the peak of atypical EAE (Fig. 5E). These data suggest that the local inflammatory microenvironment contributes to the higher expression of proinflammatory mediators in CRB-and BS-infiltrating neutrophils, compared with neutrophils from the SP.

Next, we performed a similar experiment by comparing gene expression profiles of CRB- and BS-infiltrating neutrophils between SOCS3$^{fl/fl}$ mice with classical EAE and LysMCre-SOCS3$^{fl/fl}$ mice with atypical EAE. A significant increase of CXCL2, CXCL10, iNOS, IL-1β, and TNF-α was noted (Fig. 6A). We then asked whether the proinflammatory neutrophils observed in LysMCre-SOCS3$^{fl/fl}$ mice were activated in the periphery and/or after entering the brain. Neutrophils were sorted from BM, blood, and SP of SOCS3$^{fl/fl}$ mice and LysMCre-SOCS3$^{fl/fl}$ mice throughout the course of EAE and were directly analyzed for mRNA expression. A moderate increase in CCL2 mRNA expression from neutrophils from blood and SP was observed in SOCS3$^{fl/fl}$ mice at preonset of disease, and then fluctuated during the ongoing and peak phases of disease. The levels of CCL2 in neutrophils from BM were increased at the peak of disease in SOCS3$^{fl/fl}$ mice. The expression of CCL2 in neutrophils from BM and SP was maintained at relatively stable levels during the entire disease course in LysMCre-SOCS3$^{fl/fl}$ mice, but a moderate increase of CCL2 expression was found in blood-derived neutrophils at preonset, ongoing, and peak of disease in LysMCre-SOCS3$^{fl/fl}$ mice (Fig. 6B). Interestingly, the levels of TNF-α were decreased in neutrophils from BM, blood, and SP in both SOCS3$^{fl/fl}$ mice and LysMCre-SOCS3$^{fl/fl}$ mice after the onset of disease, although a slight increase in TNF-α expression was observed in neutrophils from BM at preonset of disease in LysMCre-SOCS3$^{fl/fl}$ mice (Fig. 6B). iNOS expression was strikingly increased in neutrophils from BM, blood, and SP of both SOCS3$^{fl/fl}$ mice and LysMCre-SOCS3$^{fl/fl}$ mice starting at preonset of disease. A significantly higher level of iNOS expression was observed in BM-derived neutrophils from SOCS3$^{fl/fl}$ mice at preonset of disease compared with BM-derived neutrophils from LysMCre-SOCS3$^{fl/fl}$ mice. The levels of iNOS in BM-derived neutrophils were decreased in both SOCS3$^{fl/fl}$ and LysMCre-SOCS3$^{fl/fl}$ mice at ongoing and peak of disease. No significant difference in iNOS expression was identified in neutrophils from BM, blood, and SP of SOCS3$^{fl/fl}$

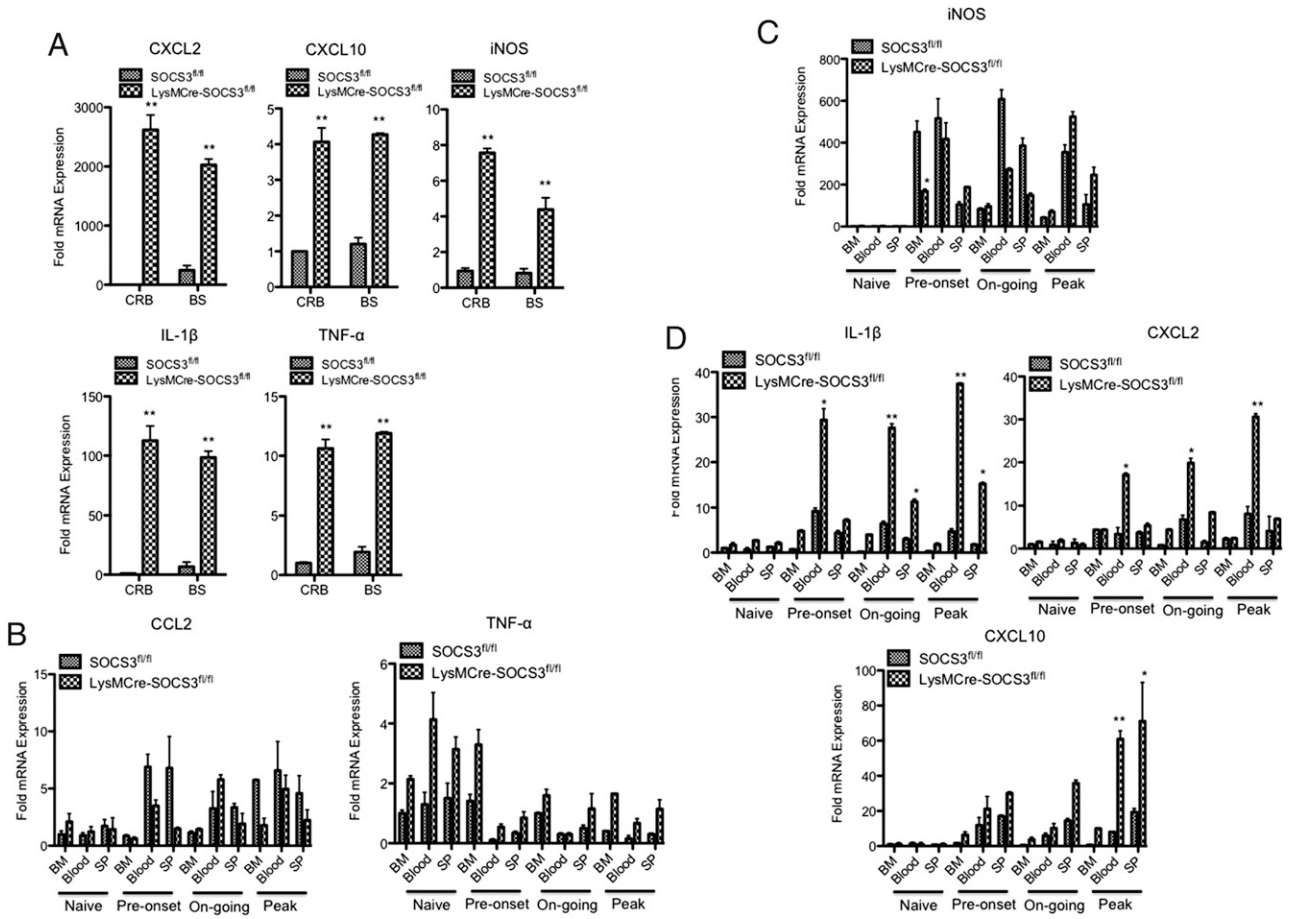

FIGURE 6. Higher expression of proinflammatory mediators from CRB- and BS-infiltrating neutrophils from LysMCre-SOCS3$^{fl/fl}$ mice with atypical EAE. (**A**) CD45^{+}CD11b^{+}Ly-6C^{low}Ly-6G^{+} neutrophils were sorted from CRB- and BS-infiltrating mononuclear cells at the peak of disease from LysMCre-SOCS3$^{fl/fl}$ mice with atypical EAE or from SOCS3$^{fl/fl}$ mice with classical EAE, mRNA isolated, and analyzed for CXCL2, CXCL10, iNOS, IL-1β, and TNF-α. Mean ± SD. Fold induction of indicated genes was compared between SOCS3$^{fl/fl}$ mice ($n = 5$) and LysMCre-SOCS3$^{fl/fl}$ mice ($n = 4$). Data represent three individual experiments. CD45^{+}CD11b^{+}Ly-6C^{low}Ly-6G^{+} neutrophils were sorted from BM, blood, and SP of LysMCre-SOCS3$^{fl/fl}$ mice with atypical EAE or from SOCS3$^{fl/fl}$ mice with classical EAE at the indicated disease stages, mRNA isolated, and analyzed for CCL2, TNF-α (**B**), iNOS (**C**), IL-1β, CXCL2, and CXCL10 (**D**). Mean ± SD ($n = 4$ mice). Data represent fold induction compared with naive SOCS3$^{fl/fl}$ BM ($n = 3$ mice in each group). $*p < 0.05$, $**p < 0.01$.

mice and LysMCre-SOCS3$^{fl/fl}$ mice at the peak of disease (Fig. 6C). In contrast, the expression levels of IL-1β and CXCL2 mRNA in blood-derived neutrophils were significantly increased at preonset, ongoing, and peak of disease in LysMCre-SOCS3$^{fl/fl}$ mice compared with SOCS3$^{fl/fl}$ mice. In addition, significantly increased levels of IL-1β were observed in SP-derived neutrophils at ongoing and peak of disease in LysMCre-SOCS3$^{fl/fl}$ mice compared with SOCS3$^{fl/fl}$ mice (Fig. 6D). Interestingly, significantly increased levels of CXCL10 in blood- and SP-derived neutrophils from LysMCre-SOCS3$^{fl/fl}$ mice were observed at the peak of disease compared with SOCS3$^{fl/fl}$ mice (Fig. 6D).

Blocking CXCR2 signaling suppresses atypical EAE development by reducing neutrophil infiltration into the CRB and BS

As CXCL2 is a major mediator in recruiting neutrophils (8, 13, 14), we used SB 225002, a selective nonpeptide inhibitor of CXCR2, the receptor for CXCL2, to investigate the effect of blocking CXCR2 signaling in the development of atypical EAE. SB 225002 treatment significantly delayed disease onset and lessened disease severity in atypical EAE (Fig. 7A, 7B). Importantly, SB 225002 treatment reduced the incidence of atypical EAE (from 60 to 25%) and increased the incidence of the mixed phenotype (from 40 to 75%) (Fig. 7A, 7B). Consistent with the reduction of atypical EAE development, blocking CXCR2 signaling significantly reduced mononuclear cell infiltration into the CRB and BS, but not into the SC (Fig. 7C). In addition, SB 225002 treatment significantly reduced the levels of neutrophils in the CRB and BS, whereas a trend for reduced neutrophil accumulation in the SC was also observed (Fig. 7D).

Overproduction of NO and axonal damage in atypical EAE

NO, which induces oxidative damage, is considered an important proinflammatory mediator involved in the pathogenesis of EAE and MS (42–45). As we observed higher mRNA level of iNOS in the CRB and BS as well as in CRB- and BS-infiltrating neutrophils from LysMCre-SOCS3$^{fl//fl}$ mice (Figs. 1D, 4E, 5B, 5E), we examined NO production in atypical EAE development. CRB-, BS-, and SC-infiltrating mononuclear cells isolated at the peak of classical EAE or atypical EAE from SOCS3$^{fl/fl}$ mice or LysMCre-SOCS3$^{fl/fl}$ mice, respectively, were cultured for 24 h, and supernatants were assayed for nitrite. A significant increase in nitrite levels was observed in supernatants from CRB-infiltrating mononuclear cells from LysMCre-SOCS3$^{fl//fl}$ mice (Fig. 8A), indicating NO may contribute to cerebellar damage in atypical EAE development. Axonal loss is the primary cause of clinical dis-

A

	EAE Incidence in LysMCre-SOCS3$^{fl/fl}$ Mice		
	Classical %	Mixed %	Atypical %
Vehicle	0	40.0	60.0
SB 225002	0	75.0*	25.0**

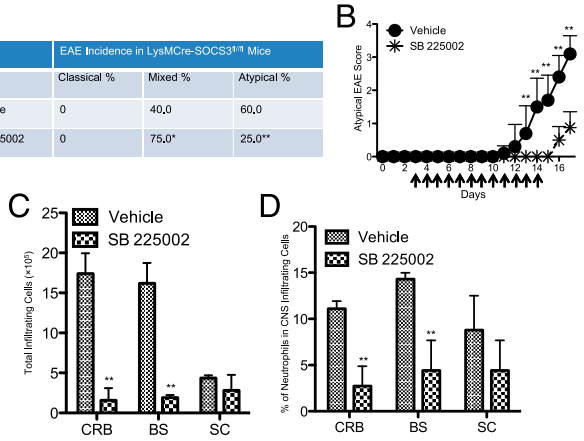

FIGURE 7. Blocking CXCR2 signaling lessens atypical EAE development by reducing neutrophil infiltration into the CRB and BS. (**A**) LysMCre-SOCS3$^{fl/fl}$ mice were administered 200 μg SB 225002 ($n = 4$) or vehicle control ($n = 5$) i.p. once per day from days 3 to 7 postimmunization and twice per day from days 8 to 14. The incidence of different EAE phenotypes was compared between the vehicle control and SB 225002-treated groups. (**B**) Mean ± SD of atypical EAE scores. Atypical EAE scores were compared between vehicle control and SB 225002 groups at the indicated time points. (**C**) Graph illustrating quantitative data for absolute numbers of total infiltrating mononuclear cells in the CRB, BS, and SC from LysMCre-SOCS3$^{fl/fl}$ mice treated with vehicle control or SB 225002 at day 17 postimmunization. Mean ± SD. (**D**) Graph illustrating quantitative data for percentage of accumulated neutrophils in total CNS-infiltrating cells from CRB, BS, and SC from LysMCre-SOCS3$^{fl/fl}$ mice treated with vehicle control or SB 225002 at day 17 postimmunization. Mean ± SD. $^*p < 0.05$, $^{**}p < 0.01$.

ability of MS and EAE (46–48). Previous studies have suggested that increased levels of NO mediate axonal degeneration (45, 49, 50); thus, we evaluated potential axonal damage in brain sections from SOCS3$^{fl/fl}$ and LysMCre-SOCS3$^{fl/fl}$ mice at the peak of classical EAE or atypical EAE disease, respectively. SMI-32 has been widely used as a marker for indication of damaged axons (51). Most strikingly, increased levels of SMI-32 staining in CRB and BS sections from LysMCre-SOCS3$^{fl/fl}$ mice were detected, compared with SOCS3$^{fl/fl}$ mice (Fig. 2C). Interestingly, most of the SMI-32–positive staining was located in the neutrophil-rich areas (Fig. 2C). Immunoblot analysis also revealed increased levels of SMI-32 from CRB lysates of LysMCre-SOCS3$^{fl/fl}$ mice at peak of disease (Fig. 8B). Thus, there is substantial axonal damage in the CRB of LysMCre-SOCS3$^{fl/fl}$ mice, which may lead to the symptoms observed in atypical EAE.

Discussion

Currently, there are multiple animal models that reflect the heterogeneity of MS pathology, helping to better understand disease pathogenesis and develop therapeutic strategies. However, no single model can recapitulate the complexity of MS in humans, indicating a clear need for developing and characterizing new animal models (52, 53). We recently demonstrated that deletion of SOCS3 in myeloid cells was associated with a particularly severe form of atypical EAE, characterized by prominent macrophage and neutrophil infiltration into the CRB, enhanced STAT3 signaling, and ataxia and tremors (3). Importantly, clinical studies from MS patients have indicated that disease affecting the CRB has a particularly poor prognosis and rapid progression, as well as significant cognitive impairment (54, 55); thus, our atypical model may represent a valuable model for the subset of MS patients with prominent CRB dysfunction.

In our previous study, we noted prominent neutrophil infiltration into the brain in LysMCre-SOCS3$^{fl//fl}$ mice with atypical EAE. As several studies suggest a correlation between neutrophil infiltration into the brain and the atypical EAE phenotype, we investigated the crucial factor(s) that determines the atypical EAE phenotype in LysMCre-SOCS3$^{fl/fl}$ mice, with an emphasis on the neutrophil population. We found that preferential infiltration and accumulation of neutrophils in the CRB are essential for the pathogenesis of atypical EAE. In addition, prominent axonal loss in the CRB is associated with the development of atypical EAE. Other atypical models share some common features with our model, including predominant involvement of the brain and prominent neutrophil infiltration (23–25, 56). However, there are also substantial differences with these other atypical models. MBP transgenic RAG$^{-/-}$ × IFN-γ$^{-/-}$ × IL-5$^{-/-}$ mice spontaneously develop a severe, atypical EAE ~50 d after birth (24), whereas our model requires immunization with MOG peptide. We immunized both SOCS3$^{fl/fl}$ mice and LysMCre-SOCS3$^{fl/fl}$ mice with OVA$_{323–339}$, an irrelevant peptide for EAE, with the same immunization protocol. No classical or atypical EAE was observed (data not shown). In addition, both SOCS3$^{fl/fl}$ and LysMCre-SOCS3$^{fl/fl}$ mice have been kept for >1 y, and no spontaneous EAE has been observed (data not shown). These data collectively indicate that MOG$_{35–55}$-specific T cells are required for atypical EAE in LysMCre-SOCS3$^{fl/fl}$ mice. Stromnes et al. (25) showed that when Th17 cells outnumbered Th1 cells in the brain, and IL-17 levels were high, C3HeB/Fej mice developed atypical EAE between 12 and 25 d after immunization. In our LysMCre-SOCS3 $^{fl/fl}$ model, there is prominent involvement of both Th1 and Th17 cells, and disease onset is more rapid (3).

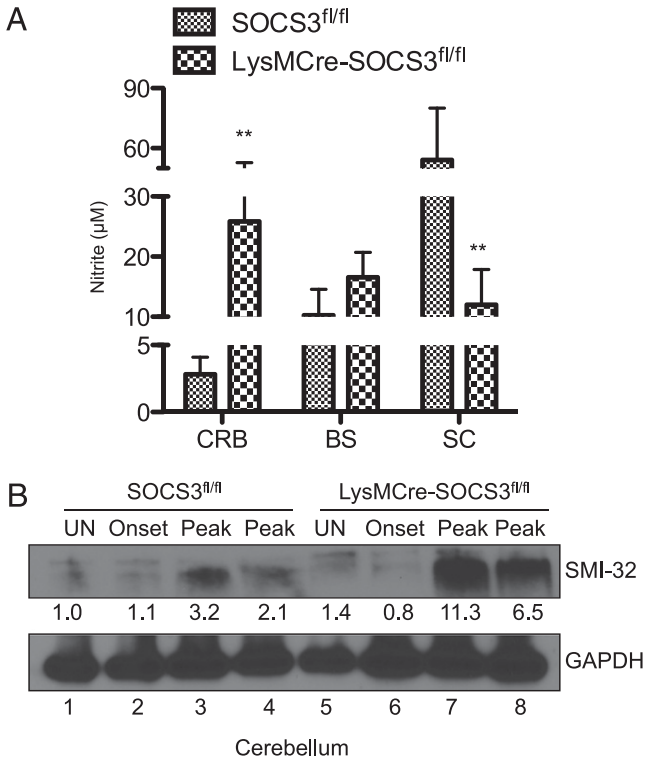

FIGURE 8. Overproduction of NO and axonal damage in atypical EAE. (**A**) CRB-, BS-, and SC-infiltrating mononuclear cells isolated at the peak of disease from SOCS3$^{fl/fl}$ mice with classical EAE or LysMCre-SOCS3$^{fl/fl}$ mice with atypical EAE were cultured for 24 h, and supernatants were analyzed for nitrite by the Griess reaction ($n = 4$ cultures/group). Mean ± SD. (**B**) Protein extracts from CRB of unimmunized (UN) or MOG$_{35–55}$-immunized SOCS3$^{fl/fl}$ with classical EAE or LysMCre-SOCS3$^{fl/fl}$ mice with atypical EAE were immunoblotted with the indicated Abs. $^{**}p < 0.01$.

Interestingly, glial fibrillary acidic protein–IL-6 transgenic mice with astrocyte-targeted production of IL-6 develop atypical EAE, characterized by severe ataxia and extensive inflammation and demyelination in the CRB with increased proportions of neutrophils (56). Disease onset in this model is similar to that in our model (~day 7), but is chronic in nature, whereas, in LysMCre-SOCS3$^{fl/fl}$ model, disease is acute and nonresolving. Activation of the IL-6/STAT3 signaling pathway in the brain may be involved in early atypical disease onset, but the lack of SOCS3 to suppress this activation is likely to contribute to the nonresolving phenotype observed in LysMCre-SOCS3 $^{fl/fl}$ mice.

Our findings are in agreement with aspects of two recent studies that showed that IFN-$\gamma R^{-/-}$ mice developed atypical EAE upon adoptive transfer of either IL-23–polarized or IL-12–polarized MOG-specific CD4$^+$ T cells (26, 27). In these studies, inflammatory demyelination was prominent in the SC, with a striking increase of macrophages/monocytes in mice with classical EAE, whereas lesion formation was identified primarily in the BS with an increase of neutrophils in mice with atypical EAE (26, 27). In addition, CXCL2 was upregulated in the brains of mice with atypical EAE (26, 27), similar to our observations. Simmons et al. (26) showed that IFN-γ inhibited CXCL2 production in the brain, but promoted its induction in the SC, whereas, in our study, we found that neutrophils contribute to the increase of CXCL2 levels in the CRB and BS.

Although correlations have been made between increased levels of neutrophils in the brain and the atypical EAE phenotype, the functional role of neutrophils in mediating this process is not clear. We provide new insight that neutrophils are functionally critical in the pathogenesis of atypical EAE in LysMCre-SOCS3$^{fl/fl}$ mice. In the inflammatory microenvironment in the CRB and BS, neutrophils secrete CXCL2 and CCL2, which may function in an autocrine and paracrine fashion to recruit neutrophils and macrophages/monocytes. In addition, neutrophils secrete IL-1β, which may stimulate astrocytes to produce CXCL2 (8, 40). More importantly, neutrophils produce NO and other mediators, including TNF-α and CXCL10, creating a proinflammatory CNS environment and directly contributing to the high levels of NO in the CRB. Furthermore, our data indicate that the proinflammatory environment in the periphery in combination with a unique inflammatory microenvironment in the CRB and BS may promote the highly proinflammatory phenotype in neutrophils from LysMCre-SOCS3$^{fl/fl}$ mice. When we depleted neutrophils in the periphery or blocked their recruitment into the CNS, a remarkable transition from atypical EAE to classical EAE or mixed EAE was observed in LysMCre-SOCS3$^{fl/fl}$ mice. Reduced levels of neutrophils in the CRB and BS accompanied the reduced atypical EAE incidence. Correlating with reduced levels of neutrophils, there were significantly decreased levels of proinflammatory mediators, including CXCL2, CCL2, CXCL10, iNOS, and IL-1β, further supporting the notion that neutrophils are functionally critical for atypical EAE development by producing these mediators.

We found that high levels of iNOS in the CRB of LysMCre-SOCS3$^{fl/fl}$ mice were associated with axonal damage and atypical EAE symptoms. Interestingly, a recent study showed that infiltrating iNOS$^+$ neutrophils contribute to ischemic brain injury, and adoptive transfer of iNOS$^{+/+}$ neutrophils is sufficient to offset, in large part, protection in iNOS$^{-/-}$ mice (57). In MS, NO is present in enhanced levels in MS lesions as a result of the activity of iNOS (58), and increased levels of NO most likely mediate axonal degeneration (45, 49, 50). Of interest, elevated levels of NO metabolites were detected in the cerebrospinal fluid during acute MS relapse, and increased levels of NO metabolites correlated with axonal degeneration and clinical disability score (59). We demonstrate upregulation of iNOS expression in CRB- and BS-infiltrating neutrophils from LysMCre-SOCS3$^{fl/fl}$ mice with atypical EAE, but not in CRB- and BS-infiltrating neutrophils from SOCS3$^{fl/fl}$ mice with classical EAE, indicating that neutrophils may have a direct role in axonal damage by producing NO. The preferential upregulation of iNOS expression in SOCS3-deficient neutrophils may be due to the proinflammatory microenvironment in the CRB and BS of LysMCre-SOCS3$^{fl/fl}$ mice during atypical EAE development.

Neutrophils have been shown to produce IL-1β to promote Th17 cell differentiation and EAE development (11). In addition, neutrophils can provide local cofactors that are required for the maturation of myeloid cells into professional APCs (9). In BALB/c mice with severe EAE, large numbers of TNF-α–secreting neutrophils were identified in the CNS, whereas only small numbers of macrophages and CD4$^+$ T cells could be detected, indicating the important role of TNF-α–secreting neutrophils in EAE (31). The Food and Drug Administration approved Tecfidera (dimethyl fumarate) in 2013 for treatment of relapsing–remitting MS (60, 61). Of interest, dimethyl fumarate reduces neurologic deficits, immune cell infiltration, and demyelination in the EAE model by interfering with neutrophil adhesion to endothelial cells and chemotaxis (62). Taken together, these data indicate that neutrophils most likely have multiple functional roles in MS and EAE.

The high levels of brain-infiltrating neutrophils are one of the most striking features observed in LysMCre-SOCS3$^{fl/fl}$ mice. In addition, high levels of neutrophils in peripheral blood were observed (data not shown). A similar phenotype was reported in an acute inflammatory arthritis model in SOCS3$^{-/\Delta vav}$ mice, which lack SOCS3 in hematopoietic and endothelial cell compartments (63). In this model, SOCS3$^{-/\Delta vav}$ mice developed a severe IL-1–dependent inflammatory arthritis, characterized by a prominent neutrophil synovial infiltrate, peripheral neutrophilia, splenomegaly, enhanced granulopoiesis, and elevated systemic levels of G-CSF and IL-6 (63). It has been reported that G-CSF promotes survival and proliferation of SOCS3-deficient granulocytes (64), and hypersensitivity of neutrophils to G-CSF could be one of the major reasons for severe joint disease. Therefore, SOCS3 may have a critical role in regulation of neutrophil responses during inflammation.

We observed that atypical EAE disease progresses rapidly after disease onset with no recovery. It has been suggested that axonal loss is one of the major determinants of progressive neurologic disability in patients with MS (46). Similarly, axonal damage is also the primary cause for permanent disability in the EAE model (47, 48). In LysMCre-SOCS3$^{fl/fl}$ mice, a prominent increase of SMI-32$^+$ axons, which is indicative of axonal damage, was observed in the CRB, and the levels of SMI-32 increased in association with increasing atypical EAE disease scores. These data indicate that axonal loss may be a characteristic hallmark of atypical EAE in LysMCre-SOCS3$^{fl/fl}$ mice, and may also explain the rapidly progressive and nonresolving disease process in atypical EAE.

In summary, this study reveals a critical role for SOCS3-deficient neutrophils and the CXCR2/CXCL2 axis in the pathogenesis of atypical EAE in LysMCre-SOCS3$^{fl/fl}$ mice. SOCS3-deficient neutrophils are hyperresponsive to cytokines such as IL-6 and G-CSF, display elevated and sustained levels of activated STAT3, and express prominent levels of iNOS, CXCL2, CCL2, CXCL10, IL-1β, and TNF-α. These cells are able to promote their own infiltration into the CRB as well as infiltration of macrophages. Depleting SOCS3-deficient neutrophils in the periphery converts the atypical EAE phenotype to mixed and classical EAE

phenotypes. Experimental data indicate that neutrophils play an important role in numerous autoimmune diseases (65); our findings in the atypical EAE model provide evidence for the importance of this cell type in EAE/MS pathogenesis.

Acknowledgments

We thank the University of Alabama at Birmingham Neuroscience Molecular Detection Core (NS47466) and the Rheumatic Diseases Core Center (P30 Flow Core) (AR48311) for advice and technical assistance. We thank Dr. Warren Alexander for the generous gift of the $SOCS3^{fl/fl}$ mice and members of the Benveniste laboratory for helpful discussions.

Disclosures

The authors have no financial conflicts of interest.

References

1. Goverman, J. 2009. Autoimmune T cell responses in the central nervous system. *Nat. Rev. Immunol.* 9: 393–407.
2. Bhat, R., and L. Steinman. 2009. Innate and adaptive autoimmunity directed to the central nervous system. *Neuron* 64: 123–132.
3. Qin, H., W.-I. Yeh, P. De Sarno, A. T. Holdbrooks, Y. Liu, M. T. Muldowney, S. L. Reynolds, L. L. Yanagisawa, T. H. I. Fox, III, K. Park, et al. 2012. Signal transducer and activator of transcription-3/suppressor of cytokine signaling-3 (STAT3/SOCS3) axis in myeloid cells regulates neuroinflammation. *Proc. Natl. Acad. Sci. USA* 109: 5004–5009.
4. Voskuhl, R. R., R. S. Peterson, B. Song, Y. Ao, L. B. Morales, S. Tiwari-Woodruff, and M. V. Sofroniew. 2009. Reactive astrocytes form scar-like perivascular barriers to leukocytes during adaptive immune inflammation of the CNS. *J. Neurosci.* 29: 11511–11522.
5. Argaw, A. T., L. Asp, J. Zhang, K. Navrazhina, T. Pham, J. N. Mariani, S. Mahase, D. J. Dutta, J. Seto, E. G. Kramer, et al. 2012. Astrocyte-derived VEGF-A drives blood-brain barrier disruption in CNS inflammatory disease. *J. Clin. Invest.* 122: 2454–2468.
6. Mayo, L., S. A. Trauger, M. Blain, M. Nadeau, B. Patel, J. I. Alvarez, I. D. Mascanfroni, A. Yeste, P. Kivisäkk, K. Kallas, et al. 2014. Regulation of astrocyte activation by glycolipids drives chronic CNS inflammation. *Nat. Med.* 20: 1147–1156.
7. McColl, S. R., M. A. Staykova, A. Wozniak, S. Fordham, J. Bruce, and D. O. Willenborg. 1998. Treatment with anti-granulocyte antibodies inhibits the effector phase of experimental autoimmune encephalomyelitis. *J. Immunol.* 161: 6421–6426.
8. Carlson, T., M. Kroenke, P. Rao, T. E. Lane, and B. Segal. 2008. The Th17-ELR + CXC chemokine pathway is essential for the development of central nervous system autoimmune disease. *J. Exp. Med.* 205: 811–823.
9. Steinbach, K., M. Piedavent, S. Bauer, J. T. Neumann, and M. A. Friese. 2013. Neutrophils amplify autoimmune central nervous system infiltrates by maturing local APCs. *J. Immunol.* 191: 4531–4539.
10. Christy, A. L., M. E. Walker, M. J. Hessner, and M. A. Brown. 2013. Mast cell activation and neutrophil recruitment promotes early and robust inflammation in the meninges in EAE. *J. Autoimmun.* 42: 50–61.
11. Yi, H., C. Guo, X. Yu, D. Zuo, and X. Y. Wang. 2012. Mouse CD11b+Gr-1+ myeloid cells can promote Th17 cell differentiation and experimental autoimmune encephalomyelitis. *J. Immunol.* 189: 4295–4304.
12. Liu, L., A. Belkadi, L. Darnall, T. Hu, C. Drescher, A. C. Cotleur, D. Padovani-Claudio, T. He, K. Choi, T. E. Lane, et al. 2010. CXCR2-positive neutrophils are essential for cuprizone-induced demyelination: relevance to multiple sclerosis. *Nat. Neurosci.* 13: 319–326.
13. Semple, B. D., T. Kossmann, and M. C. Morganti-Kossmann. 2010. Role of chemokines in CNS health and pathology: a focus on the CCL2/CCR2 and CXCL8/CXCR2 networks. *J. Cereb. Blood Flow Metab.* 30: 459–473.
14. Nygårdas, P. T., J. A. Määttä, and A. E. Hinkkanen. 2000. Chemokine expression by central nervous system resident cells and infiltrating neutrophils during experimental autoimmune encephalomyelitis in the BALB/c mouse. *Eur. J. Immunol.* 30: 1911–1918.
15. Naegele, M., K. Tillack, S. Reinhardt, S. Schippling, R. Martin, and M. Sospedra. 2012. Neutrophils in multiple sclerosis are characterized by a primed phenotype. *J. Neuroimmunol.* 242: 60–71.
16. Ishizu, T., M. Osoegawa, F. J. Mei, H. Kikuchi, M. Tanaka, Y. Takakura, M. Minohara, H. Murai, F. Mihara, T. Taniwaki, and J. Kira. 2005. Intrathecal activation of the IL-17/IL-8 axis in opticospinal multiple sclerosis. *Brain* 128: 988–1002.
17. Lucchinetti, C. F., R. N. Mandler, D. McGavern, W. Bruck, G. Gleich, R. M. Ransohoff, C. Trebst, B. Weinshenker, D. Wingerchuk, J. E. Parisi, and H. Lassmann. 2002. A role for humoral mechanisms in the pathogenesis of Devic's neuromyelitis optica. *Brain* 125: 1450–1461.
18. Rumble, J. M., A. K. Huber, G. Krishnamoorthy, A. Srinivasan, D. A. Giles, X. Zhang, L. Wang, and B. M. Segal. 2015. Neutrophil-related factors as biomarkers in EAE and MS. *J. Exp. Med.* 212: 23–35.
19. Breij, E. C., B. P. Brink, R. Veerhuis, C. van den Berg, R. Vloet, R. Yan, C. D. Dijkstra, P. van der Valk, and L. Bö. 2008. Homogeneity of active demyelinating lesions in established multiple sclerosis. *Ann. Neurol.* 63: 16–25.
20. Metz, I., S. D. Weigand, B. F. Popescu, J. M. Frischer, J. E. Parisi, Y. Guo, H. Lassmann, W. Brück, and C. F. Lucchinetti. 2014. Pathologic heterogeneity persists in early active multiple sclerosis lesions. *Ann. Neurol.* 75: 728–738.
21. Amezcua, L., A. Lerner, K. Ledezma, D. Conti, M. Law, L. Weiner, and A. Langer-Gould. 2013. Spinal cord lesions and disability in Hispanics with multiple sclerosis. *J. Neurol.* 260: 2770–2776.
22. Raine, C. S., L. B. Barnett, A. Brown, T. Behar, and D. E. McFarlin. 1980. Neuropathology of experimental allergic encephalomyelitis in inbred strains of mice. *Lab. Invest.* 43: 150–157.
23. Bettelli, E., B. Sullivan, S. J. Szabo, R. A. Sobel, L. H. Glimcher, and V. K. Kuchroo. 2004. Loss of T-bet, but not STAT1, prevents the development of experimental autoimmune encephalomyelitis. *J. Exp. Med.* 200: 79–87.
24. Wensky, A. K., G. C. Furtado, M. C. Marcondes, S. Chen, D. Manfra, S. A. Lira, D. Zagzag, and J. J. Lafaille. 2005. IFN-gamma determines distinct clinical outcomes in autoimmune encephalomyelitis. *J. Immunol.* 174: 1416–1423.
25. Stromnes, I. M., L. M. Cerretti, D. Liggitt, R. A. Harris, and J. M. Goverman. 2008. Differential regulation of central nervous system autoimmunity by $T_{(H)}1$ and $T_{(H)}17$ cells. *Nat. Med.* 14: 337–342.
26. Simmons, S. B., D. Liggitt, and J. M. Goverman. 2014. Cytokine-regulated neutrophil recruitment is required for brain but not spinal cord inflammation during experimental autoimmune encephalomyelitis. *J. Immunol.* 193: 555–563.
27. Stoolman, J. S., P. C. Duncker, A. K. Huber, and B. M. Segal. 2014. Site-specific chemokine expression regulates central nervous system inflammation and determines clinical phenotype in autoimmune encephalomyelitis. *J. Immunol.* 193: 564–570.
28. Mantovani, A., M. A. Cassatella, C. Costantini, and S. Jaillon. 2011. Neutrophils in the activation and regulation of innate and adaptive immunity. *Nat. Rev. Immunol.* 11: 519–531.
29. Werner, J. L., M. A. Gessner, L. M. Lilly, M. P. Nelson, A. E. Metz, D. Horn, C. W. Dunaway, J. Deshane, D. D. Chaplin, C. T. Weaver, et al. 2011. Neutrophils produce interleukin 17A (IL-17A) in a dectin-1- and IL-23-dependent manner during invasive fungal infection. *Infect. Immun.* 79: 3966–3977.
30. Zindl, C. L., J. F. Lai, Y. K. Lee, C. L. Maynard, S. N. Harbour, W. Ouyang, D. D. Chaplin, and C. T. Weaver. 2013. IL-22-producing neutrophils contribute to antimicrobial defense and restitution of colonic epithelial integrity during colitis. *Proc. Natl. Acad. Sci. USA* 110: 12768–12773.
31. Määttä, J. A., U. R. Sjöholm, P. T. Nygårdas, A. A. Salmi, and A. E. Hinkkanen. 1998. Neutrophils secreting tumor necrosis factor alpha infiltrate the central nervous system of BALB/c mice with experimental autoimmune encephalomyelitis. *J. Neuroimmunol.* 90: 162–175.
32. Ryan, S. O., J. L. Johnson, and B. A. Cobb. 2013. Neutrophils confer T cell resistance to myeloid-derived suppressor cell-mediated suppression to promote chronic inflammation. *J. Immunol.* 190: 5037–5047.
33. Croker, B. A., D. L. Krebs, J.-G. Zhang, S. Wormald, T. A. Willson, E. G. Stanley, L. Robb, C. J. Greenhalgh, I. Förster, B. E. Clausen, et al. 2003. SOCS3 negatively regulates IL-6 signaling *in vivo*. *Nat. Immunol.* 4: 540–545.
34. Liu, Y., A. T. Holdbrooks, P. De Sarno, A. L. Rowse, L. L. Yanagisawa, B. C. McFarland, L. E. Harrington, C. Raman, S. Sabbaj, E. N. Benveniste, and H. Qin. 2014. Therapeutic efficacy of suppressing the Jak/STAT pathway in multiple models of experimental autoimmune encephalomyelitis. *J. Immunol.* 192: 59–72.
35. Bento, A. F., D. F. Leite, R. F. Claudino, D. B. Hara, P. C. Leal, and J. B. Calixto. 2008. The selective nonpeptide CXCR2 antagonist SB225002 ameliorates acute experimental colitis in mice. *J. Leukoc. Biol.* 84: 1213–1221.
36. Baker, B. J., K. W. Park, H. Qin, X. Ma, and E. N. Benveniste. 2010. IL-27 inhibits OSM-mediated TNF-α and iNOS gene expression in microglia. *Glia* 58: 1082–1093.
37. Ritzman, A. M., J. M. Hughes-Hanks, V. A. Blaho, L. E. Wax, W. J. Mitchell, and C. R. Brown. 2010. The chemokine receptor CXCR2 ligand KC (CXCL1) mediates neutrophil recruitment and is critical for development of experimental Lyme arthritis and carditis. *Infect. Immun.* 78: 4593–4600.
38. Dogan, R. N., A. Elhofy, and W. J. Karpus. 2008. Production of CCL2 by central nervous system cells regulates development of murine experimental autoimmune encephalomyelitis through the recruitment of TNF- and iNOS-expressing macrophages and myeloid dendritic cells. *J. Immunol.* 180: 7376–7384.
39. Perrin, P. J., C. A. Rumbley, R. L. Beswick, E. Lavi, and S. M. Phillips. 2000. Differential cytokine and chemokine production characterizes experimental autoimmune meningitis and experimental autoimmune encephalomyelitis. *Clin. Immunol.* 94: 114–124.
40. Chou, R. C., N. D. Kim, C. D. Sadik, E. Seung, Y. Lan, M. H. Byrne, B. Haribabu, Y. Iwakura, and A. D. Luster. 2010. Lipid-cytokine-chemokine cascade drives neutrophil recruitment in a murine model of inflammatory arthritis. *Immunity* 33: 266–278.
41. Yoshimura, T., and M. Takahashi. 2007. IFN-gamma-mediated survival enables human neutrophils to produce MCP-1/CCL2 in response to activation by TLR ligands. *J. Immunol.* 179: 1942–1949.
42. Sarchielli, P., A. Orlacchio, F. Vicinanza, G. P. Pelliccioli, M. Tognoloni, C. Saccardi, and V. Gallai. 1997. Cytokine secretion and nitric oxide production by mononuclear cells of patients with multiple sclerosis. *J. Neuroimmunol.* 80: 76–86.
43. Acar, G., F. Idiman, E. Idiman, G. Kirkali, H. Cakmakçi, and S. Ozakbaş. 2003. Nitric oxide as an activity marker in multiple sclerosis. *J. Neurol.* 250: 588–592.
44. Rejdak, K., M. J. Eikelenboom, A. Petzold, E. J. Thompson, Z. Stelmasiak, R. H. Lazeron, F. Barkhof, C. H. Polman, B. M. Uitdehaag, and G. Giovannoni. 2004. CSF nitric oxide metabolites are associated with activity and progression of multiple sclerosis. *Neurology* 63: 1439–1445.

45. Redford, E. J., R. Kapoor, and K. J. Smith. 1997. Nitric oxide donors reversibly block axonal conduction: demyelinated axons are especially susceptible. *Brain* 120: 2149–2157.
46. Bjartmar, C., J. R. Wujek, and B. D. Trapp. 2003. Axonal loss in the pathology of MS: consequences for understanding the progressive phase of the disease. *J. Neurol. Sci.* 206: 165–171.
47. Wujek, J. R., C. Bjartmar, E. Richer, R. M. Ransohoff, M. Yu, V. K. Tuohy, and B. D. Trapp. 2002. Axon loss in the spinal cord determines permanent neurological disability in an animal model of multiple sclerosis. *J. Neuropathol. Exp. Neurol.* 61: 23–32.
48. van Waesberghe, J. H., W. Kamphorst, C. J. De Groot, M. A. van Walderveen, J. A. Castelijns, R. Ravid, G. J. Lycklama à Nijeholt, P. van der Valk, C. H. Polman, A. J. Thompson, and F. Barkhof. 1999. Axonal loss in multiple sclerosis lesions: magnetic resonance imaging insights into substrates of disability. *Ann. Neurol.* 46: 747–754.
49. Kapoor, R., M. Davies, P. A. Blaker, S. M. Hall, and K. J. Smith. 2003. Blockers of sodium and calcium entry protect axons from nitric oxide-mediated degeneration. *Ann. Neurol.* 53: 174–180.
50. Smith, K. J., R. Kapoor, S. M. Hall, and M. Davies. 2001. Electrically active axons degenerate when exposed to nitric oxide. *Ann. Neurol.* 49: 470–476.
51. Soulika, A. M., E. Lee, E. McCauley, L. Miers, P. Bannerman, and D. Pleasure. 2009. Initiation and progression of axonopathy in experimental autoimmune encephalomyelitis. *J. Neurosci.* 29: 14965–14979.
52. Pachner, A. R. 2011. Experimental models of multiple sclerosis. *Curr. Opin. Neurol.* 24: 291–299.
53. Attfield, K. E., C. A. Dendrou, and L. Fugger. 2012. Bridging the gap from genetic association to functional understanding: the next generation of mouse models of multiple sclerosis. *Immunol. Rev.* 248: 10–22.
54. Davie, C. A., G. J. Barker, S. Webb, P. S. Tofts, A. J. Thompson, A. E. Harding, W. I. McDonald, and D. H. Miller. 1995. Persistent functional deficit in multiple sclerosis and autosomal dominant cerebellar ataxia is associated with axon loss. *Brain* 118: 1583–1592.
55. Naismith, R. T., K. Trinkaus, and A. H. Cross. 2006. Phenotype and prognosis in African-Americans with multiple sclerosis: a retrospective chart review. *Mult. Scler.* 12: 775–781.
56. Quintana, A., M. Müller, R. F. Frausto, R. Ramos, D. R. Getts, E. Sanz, M. J. Hofer, M. Krauthausen, N. J. King, J. Hidalgo, and I. L. Campbell. 2009. Site-specific production of IL-6 in the central nervous system retargets and enhances the inflammatory response in experimental autoimmune encephalomyelitis. *J. Immunol.* 183: 2079–2088.
57. Garcia-Bonilla, L., J. M. Moore, G. Racchumi, P. Zhou, J. M. Butler, C. Iadecola, and J. Anrather. 2014. Inducible nitric oxide synthase in neutrophils and endothelium contributes to ischemic brain injury in mice. *J. Immunol.* 193: 2531–2537.
58. Bö, L., T. M. Dawson, S. Wesselingh, S. Mörk, S. Choi, P. A. Kong, D. Hanley, and B. D. Trapp. 1994. Induction of nitric oxide synthase in demyelinating regions of multiple sclerosis brains. *Ann. Neurol.* 36: 778–786.
59. Rejdak, K., A. Petzold, Z. Stelmasiak, and G. Giovannoni. 2008. Cerebrospinal fluid brain specific proteins in relation to nitric oxide metabolites during relapse of multiple sclerosis. *Mult. Scler.* 14: 59–66.
60. Fox, R. J., D. H. Miller, J. T. Phillips, M. Hutchinson, E. Havrdova, M. Kita, M. Yang, K. Raghupathi, M. Novas, M. T. Sweetser, et al. 2012. Placebo-controlled phase 3 study of oral BG-12 or glatiramer in multiple sclerosis. *N. Engl. J. Med.* 367: 1087–1097.
61. Gold, R., L. Kappos, D. L. Arnold, A. Bar-Or, G. Giovannoni, K. Selmaj, C. Tornatore, M. T. Sweetser, M. Yang, S. I. Sheikh, K. T. Dawson, et al. 2012. Placebo-controlled phase 3 study of oral BG-12 for relapsing multiple sclerosis. *N. Engl. J. Med.* 367: 1098–1107.
62. Chen, H., J. C. Assmann, A. Krenz, M. Rahman, M. Grimm, C. M. Karsten, J. Köhl, S. Offermanns, N. Wettschureck, and M. Schwaninger. 2014. Hydroxycarboxylic acid receptor 2 mediates dimethyl fumarate's protective effect in EAE. *J. Clin. Invest.* 124: 2188–2192.
63. Wong, P. K., P. J. Egan, B. A. Croker, K. O'Donnell, N. A. Sims, S. Drake, H. Kiu, E. J. McManus, W. S. Alexander, A. W. Roberts, and I. P. Wicks. 2006. SOCS-3 negatively regulates innate and adaptive immune mechanisms in acute IL-1-dependent inflammatory arthritis. *J. Clin. Invest.* 116: 1571–1581.
64. Croker, B. A., D. Metcalf, L. Robb, W. Wei, S. Mifsud, L. DiRago, L. A. Cluse, K. D. Sutherland, L. Hartley, E. Williams, et al. 2004. SOCS3 is a critical physiological negative regulator of G-CSF signaling and emergency granulopoiesis. *Immunity* 20: 153–165.
65. Németh, T., and A. Mócsai. 2012. The role of neutrophils in autoimmune diseases. *Immunol. Lett.* 143: 9–19.